JARQ 60 (1), 97-109 (2026) https://www.jircas.go.jp

Potential for Identifying Phytoplankton Communities, Including Harmful Dinoflagellate *Karenia* Blooms, Using an *in-situ* Multi-Wavelength Excitation Fluorometer

Yukiko TANIUCHI[1]*, Taketoshi KODAMA[2,4] and Yutaka OKUMURA[3]

[1] Fisheries Resources Institute (Kushiro Station), Japan Fisheries Research and Education Agency, Kushiro, Japan
[2] Fisheries Resources Institute (Yokohama Station), Japan Fisheries Research and Education Agency, Yokohama, Japan
[3] Fisheries Resources Institute (Shiogama Station), Japan Fisheries Research and Education Agency, Shiogama, Japan

Abstract

A multi-excitation fluorometer, the Multi-Exciter (MEX), is designed to identify phytoplankton composition based on the fluorescence provided by nine different excitation wavelengths. The phytoplankton community structure was monitored using MEX off the coast of eastern Hokkaido, Japan, from 2019 to 2021, encompassing the period of an outbreak of the harmful dinoflagellate *Karenia* spp. (*Karenia selliformis*, *K. mikimotoi*, and *K. longicanalis*) in autumn 2021. MEX could distinguish the vertical structure of spring diatom blooms but not that of dinoflagellate blooms in October 2021. This is possibly because MEX identified peridinin-type dinoflagellates, whereas *Karenia* spp. lacked peridinin. The *Karenia* index was defined based on the similarities in fluorescence properties (36 combinations of the ratio of fluorescence values obtained using MEX) of representative *Karenia* bloom water, aiming to overcome this misidentification. High *Karenia* indices were observed at depths of 1 m-20 m in October 2021. This implied that *Karenia* spp. were distributed at depths of < 20 m during their blooms, and MEX detected *Karenia* blooms with their vertical structure. No *Karenia* spp. were observed using microscopy in May 2021; however, high *Karenia* indices were observed in the subsurface. Hence, the fluorometric approach is a simple and rapid method for identifying distinguishing events in the phytoplankton community when combined with sporadic microscopic observations.

Disciplines: Fisheries
Additional key words: harmful algal bloom, *Karenia selliformis*

Introduction

Phytoplankton blooms in the ocean fix substantial amounts of carbon dioxide and become energy sources for fisheries (Platt et al. 2003, Koeller et al. 2009). However, blooms of harmful phytoplankton damage fisheries and aquaculture (GEOHAB 2010). Therefore, monitoring both the abundance and composition of phytoplankton is essential for understanding carbon fluxes and the marine environment of fishing fields and reducing damage from harmful phytoplankton blooms.

Outbreaks of harmful dinoflagellates, namely *Karenia* spp. (termed *Karenia* outbreaks), occurred in the northwest Pacific, off the coast of eastern Hokkaido, the northernmost of Japan's four main islands, in 2021 (Iwataki et al. 2022), causing extensive damage to local marine fauna (Hasegawa et al. 2022, Yao & Noda 2023, Johnstone et al. 2024). The damage to fisheries was estimated at > 9.7 billion JPY by the Hokkaido Prefectural government (Hokkaido Prefecture, published 30 September 2023, https://www.pref.hokkaido.lg.jp/sr/sky/akashio_info.html), which is the worst on record in Japan.

*Corresponding author: taniuchi_yukiko80@fra.go.jp
[4] Present address: Graduate School of Agricultural and Life Sciences, The University of Tokyo, Tokyo, Japan
Received 26 August 2024; accepted 5 June 2025; J-STAGE Advanced Epub 20 October 2025.
https://doi.org/10.6090/jarq.24S30

Red tides of *Karenia* spp. (especially *K. mikimotoi*) are frequently reported in western Japan. Among the red tide species that caused damage to fisheries between 1970 and 2000, the number of red tides caused by *K. mikimotoi* was the highest (Sakamoto et al. 2021). In Hokkaido, *K. mikimotoi* red tides were first recorded in Hakodate Bay in 2015 (Shimada et al. 2016, Kakumu et al. 2018). Subsequently, *K. mikimotoi* red tides were reported in Hakodate Bay and Funka Bay in 2021 and 2022, respectively (Natsuike et al. 2023). The Tsushima Current, which is derived from the Kuroshio, flows northward in the Sea of Japan off the west coast of Hokkaido. The Tsushima Current flows out of the Tsugaru Strait in southern Hokkaido and becomes the Tsugaru Warm Current (Fig. 1A). It has been suggested that the *K. mikimotoi* found in Hakodate Bay and Funka Bay may originate from certain populations of *K. mikimotoi* blooms in western Japan, which are transported by the Tsushima Warm Current and Tsugaru Warm Current (Shimada et al. 2016, Natsuike et al. 2023). The Tsushima Warm Current flows out of the Soya Strait into the Okhotsk Sea and becomes the Soya Warm Current (Fig. 1A). *K. mikimotoi* red tides have not yet occurred on the coast of the Okhotsk Sea in Hokkaido; however, *K. mikimotoi* has been detected using metagenetic analyses (Sildever et al. 2019). This suggests that the distribution of *K. mikimotoi* has expanded to northern Japan.

The dominant species in the *Karenia* outbreaks in 2021 was *K. selliformis*, the bloom of which was first recorded in Japan at that time (Iwataki et al. 2022). The

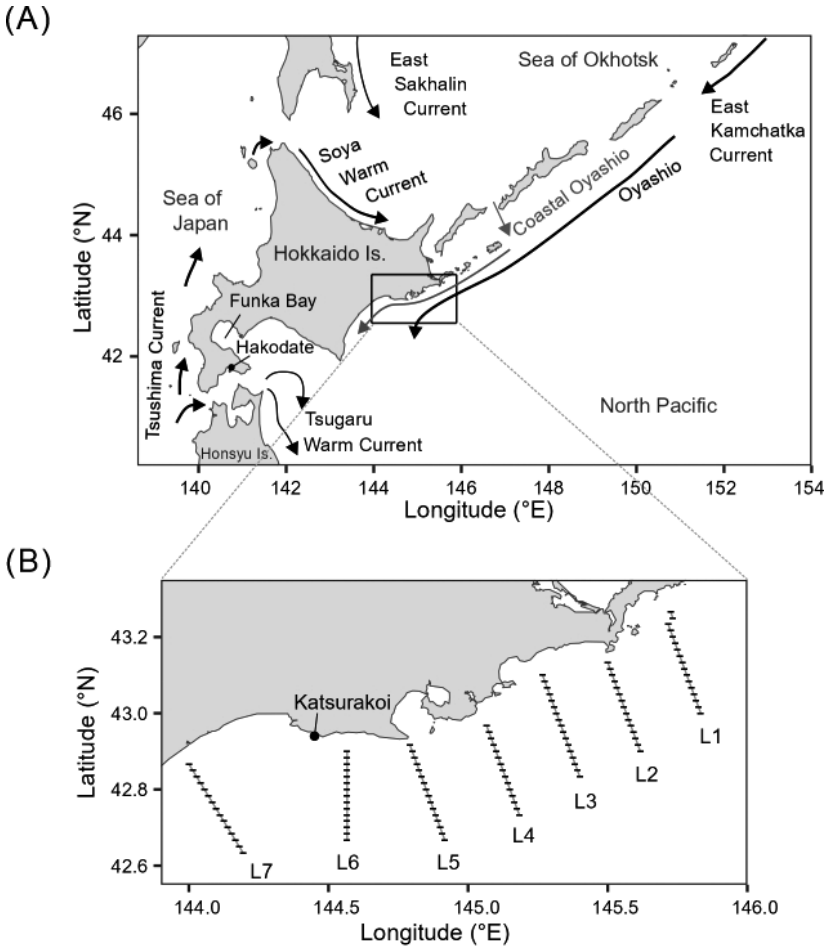

Fig. 1. Observation map

(A) Arrows show surface currents around Hokkaido, Japan. (B) The stations where phytoplankton composition was monitored using a multi-wavelength excitation fluorometer during 2019-2021 are shown as short bars. The black circle indicates the Katsurakoi fishing port where the *Karenia* bloom water was collected on 2 November 2021.

other co-occurring species were *K. mikimotoi* and *K. longicanalis* (Iwataki et al. 2022). A bloom of several co-occurring species of *Karenia* was also reported off the coast of Kamchatka, Russia, in 2020 (Orlova et al. 2022, Alexanin et al. 2023). The sequence of the ribosomal DNA (rDNA) gene of *K. selliformis* isolated from the *Karenia* outbreak was identical to that of *K. selliformis* from Kamchatka (Iwataki et al. 2022). In contrast, the rDNA sequences of *K. mikimotoi* and *K. longicanalis* were identical to those of western Japan, but not to those of Kamchatka (Iwataki et al. 2022). Kuroda et al. (2021) applied particle-tracking simulations and showed three possibilities for the origin of *Karenia* spp. in *Karenia* outbreaks in Hokkaido: east of the Kamchatka Peninsula, the Sea of Japan, and east of Sakhalin Island in the Okhotsk Sea. Miyazono & Kuroda (2024) suggested that *Karenia* spp. blooms on the coast of Kamchatka in 2020 were transported and developed the initial community off eastern Hokkaido and insisted on the importance of monitoring *Karenia* spp. offshore.

The presence of *Karenia* spp. in the outbreaks has been confirmed using microscopic observations (Yamaguchi et al. 2022, Taniuchi et al. 2023) and marker gene detection (Iwataki et al. 2022, Orlova et al. 2022). Such methods provide accurate, dependable information on the presence of *Karenia* spp. but are time- and labor-intensive for monitoring large areas. Satellite observations of ocean color were used to detect the horizontal distribution of the bloom during the *Karenia* outbreak in 2021 (Kuroda et al. 2021) and showed that the outbreak was approximately 300 km wide (Kuroda et al. 2022). However, satellite observations could not show the vertical distribution (Bjørnsen & Nielsen 1991, Miyamura 2016). *Karenia* spp. exhibit diel vertical migration and accumulate at high cell densities in the subsurface depths during the daytime (Honjo et al. 1990, Yamaguchi 1994, Koizumi et al. 1996, Miyamura 2016), resulting in changes in the environment (Honjo et al. 1990, Yamaguchi 1994, Miyamura 2016, Shikata et al. 2017). Therefore, red tides may be overlooked when using surface monitoring, such as ocean color. Information on their vertical distribution is essential for monitoring *Karenia* spp.

The Harmful Algal Indication sensor (HAI sensor, JFE-Advantech, Hyogo, Japan) was used to detect different peak wavelengths of the chlorophyll fluorescence spectra and distinguish *K. mikimotoi* and *Chattonella marina* var. antiqua from other phytoplankton (Yoshida et al. 2021). Although it helps monitor red tide plankton, its disadvantage is that it is not versatile enough for other applications. The Multi-Exciter (MEX:JFE-Advantech, Hyogo, Japan) is a multi-excitation fluorometer that can help reveal community composition based on the fluorescence characteristics of phytoplankton through semi-real-time observations (Yoshida et al. 2011). Nine light-emitting diode (LED) light sources in MEX excite matter in water (at wavelengths of 375, 400, 420, 435, 470, 505, 525, 570, and 590 nm), and MEX detects the emitted fluorescence. The fluorescence pattern of *Karenia* spp. has not been previously reported, but *Karenia* spp. have unique photosynthetic pigments, such as gyroxanthin-diester (Örnólfsdóttir et al. 2003). *Karenia* blooms show a slightly different light absorption (Millie et al. 1997); thus, their fluorescent properties are expected to be unique, and MEX observation is a potentially useful method to identify the distribution of *Karenia* spp. blooms. If MEX enables the monitoring of *Karenia* spp., it will allow simultaneous monitoring of *Karenia* in parallel with regular phytoplankton monitoring.

The Japan Fisheries Research and Education Agency has monitored the marine environment off southeastern Hokkaido since 2015, and MEX observations began in 2019. The observations were conducted in seven lines with 15-17 stations spaced one mile apart to capture the sub-mesoscale marine environment along the Pacific coast of eastern Hokkaido in both the east-west and offshore directions. The monitoring period included the *Karenia* outbreak in 2021 (e.g., Kuroda et al. 2022, Taniuchi et al. 2023). In this study, we measured the phytoplankton community structure from 2019 to 2021 off southeastern Hokkaido using MEX and aimed to 1) evaluate the ability of MEX to routinely monitor the phytoplankton community structure and 2) detect the vertical distribution of *Karenia* outbreaks in 2021 along the coast of eastern Hokkaido.

Materials and methods

1. Observations

(1) Monitoring of L-lines

Field observations were conducted from October 2019 to October 2021 by R/V *Hokko-maru* and R/V *Wakataka-maru* in the high-resolution monitoring lines, termed the "L-lines" off the coast of eastern Hokkaido (Fig. 1). The observations were conducted in January, May, and October (Table 1) from 02:30 to 21:00 in May, and from 04:00 to 22:00 in January and October.

MEX (MFL50W-USB, JFE Advantech Co., Ltd., Hyogo, Japan) observations were conducted at all observation stations along the L-line. The MEX was fixed to a conductivity-temperature-depth (CTD) sensor (Sea-Bird Electronics 911plus CTD system; Sea-Bird Electronics, Inc., Bellevue, WA, USA). The observation depth was from the surface to 490 m, or near the seafloor. As the detection of *Karenia* spp. was attempted in parallel

with the regular monitoring of phytoplankton species composition, the instrument was not customized in this study.

(2) Observation of the *Karenia* bloom water

Water samples were collected on 2 November 2021, from the Katsurakoi fishing port (42.944° N, 144.446° E; Fig. 1B) to collect data on the *Karenia* spp. bloom. Surface-water samples were collected in a bucket and brought back to the laboratory. The samples were placed in a black shaded bucket, and MEX observation was performed for approximately five minutes. The observation data were used as the reference data for *Karenia* spp.

(3) Enumeration of *Karenia* spp. and HPLC analysis

Water samples (0.5 L-1 L) to enumerate *Karenia* spp. were collected using a CTD rosette equipped with Niskin bottles (Sea-Bird Electronics 911plus CTD system; Sea-Bird Electronics, Inc.) at a depth of 10 m or a bucket to collect surface water. Water samples were fixed with acid Lugol's solution (final concentration, 4%) and concentrated to 25 mL-50 mL using reverse filtration through 2 μm pore size filters (Dodson & Thomas 1964). *Karenia* spp. were identified under a light microscope (ECLIPSE TE300; Nikon, Tokyo, Japan) according to the taxonomy described by Iwataki et al. (2022). The limit of detection was 50 cells L^{-1}.

For HPLC analysis, 20 mL-500 mL of water samples were filtered with a 25 mm GF/F filter (Cytiva, Tokyo, Japan) under approximately 0.01 MPa and frozen (−80°C) in the dark. Phytoplankton pigments were extracted and measured using an HPLC system (Shimadzu, Kyoto, Japan) as described by Kodama et al. (2022). Phytoplankton pigments were analyzed according to the protocol described by Zapata et al. (2000).

Table 1. MEX observation dates

Year	Month	Day	Line or Station
2019	10	7	L1, L2
		8	L3, L4
		9	L7
		10	L5, L6
2020	1	25	L7
		26	L3, L5
		27	L1
2020	5	19	L1, L3
		20	L3, L4
2020	10	14	L7
		15	L5, L6
		16	L1, L2
		17	L3, L4
2021	1	24	L7
		25	L1, L3
		26	L5
2021	5	18	L5
		19	L3, L4
		20	L6, L7
2021	10	10	L6, L7
		12	L1, L2
		13	L3, L4
		14	L5
2021	11	2	Katsurakoi port

2. MEX data analysis

Because the samples collected at 0 m sometimes contained air that influenced the readings, they were omitted from the analysis. The settings for MEX are as described by Kodama et al. (2022). The binary data recorded in MEX were transformed into numerical values using the default MEX software (MFL Software, JFE-Advantech, Hyogo, Japan). The fluorescence values given by the 435 and 470 nm excitations showed a strong correlation with Chlorophyll (Chl.) *a* concentration (Kodama et al. 2022). Chl. *a* concentration was estimated from the fluorescence value given by 435 nm excitation.

Species composition estimation using MEX was performed by conducting multiple regression analysis on the fluorescence excitation spectrum obtained in situ with the fluorescence excitation spectrum of known phytoplankton normalized using the Chl. *a* concentration as the base spectrum (Yoshida et al. 2011). Kodama et al. (2022) reported that a more accurate estimation of taxonomic composition is possible by decomposing the MEX fluorescence value using a linear inverse model and the reference database in Kodama et al. (2022) and calculating the coefficients. The phytoplankton composition was then reconstructed using the coefficients and the phytoplankton pigments of the reference data, which were analyzed using HPLC. In this study, the species composition of the five phytoplankton groups (cryptophytes, dinoflagellates, diatoms, cyanophytes, and other phytoplankton) was determined as described by Kodama et al. (2022). The phytoplankton composition analysis was conducted on the L3-line, where most of the data were available. As the Chl. *a* concentration was not necessary for identifying *Karenia* blooms, the ratio of the fluorescence values was used to compare the field and representative *Karenia* bloom waters. In total, 36 combinations were obtained for the ratios of fluorescence values. The *Karenia* bloom fluorescence ratio was based on the median fluorescence values of representative

Karenia bloom waters in Katsurakoi (Fig. 2). There were also 36 combinations of the fluorescence values for the fluorescence ratio of the L-line data. The correlation coefficients (r) between the *Karenia* bloom fluorescence ratio and the fluorescence ratio of the L-line data were calculated. The similarities were evaluated using correlation coefficients (r). Because the r values were expected to be high where red tides had occurred, we defined the index as follows:

$$\textit{Karenia}\ \text{index} = -\log_{10}(1-r) \quad \ldots(1)$$

where *Karenia* indices = 1, 2, and 3 indicate r of 0.9, 0.99, and 0.999, respectively. The median and interquartile range (IQR) of the *Karenia* indices were 3.431 and 0.765 in the representative *Karenia* bloom water, respectively. We defined a high *Karenia* index as follows: > median – 1.5 × IQR, 2.28, which is conventionally used as an index for the detection of outlier values.

The euphotic layer was defined as the layer where light penetration was 1% of that on the surface; it was calculated based on the attenuation coefficient at 490 nm (kd_{490}). The kd_{490} value was obtained from the Global Ocean Color (Copernicus GlobColor; product ID: OCEANCOLOUR_GLO_BGC_L4_MY_009_104).

Results

1. Distribution of Chl. *a*

The Chl. *a* concentrations and their vertical profiles showed seasonality (Fig. 3). In January, Chl. *a* concentrations were low (< 3 mg m^{-3}), and the subsurface chlorophyll maximum was unclear. In May, the maximum Chl. *a* was observed in the subsurface layer (depth of 10 m-35 m). The highest Chl. *a* concentration was 11.8 mg m^{-3} at St. L7-10 in May 2021. No clear east-west differences were observed in the Chl. *a* concentrations in May, and Chl. *a* concentration in the offshore area was higher than that in the coastal areas. The Chl. *a* concentrations in October varied depending on the year. In 2019, the Chl. *a* concentrations were < 1.5 mg m^{-3} throughout the area. In 2020, the Chl. *a* concentrations ranged from 2 to 4 mg m^{-3} in the surface layer at many stations. Chl. *a* concentrations were high at the western stations, and extremely high Chl. *a* concentrations (> 5 mg m^{-3}) was observed at the L7-line. Chl. *a* concentrations were > 3 mg m^{-3} at almost all stations, and the maximum Chl. *a* concentration (14.7 mg m^{-3}) was observed at station L5-10 when the *Karenia* outbreak occurred in October 2021.

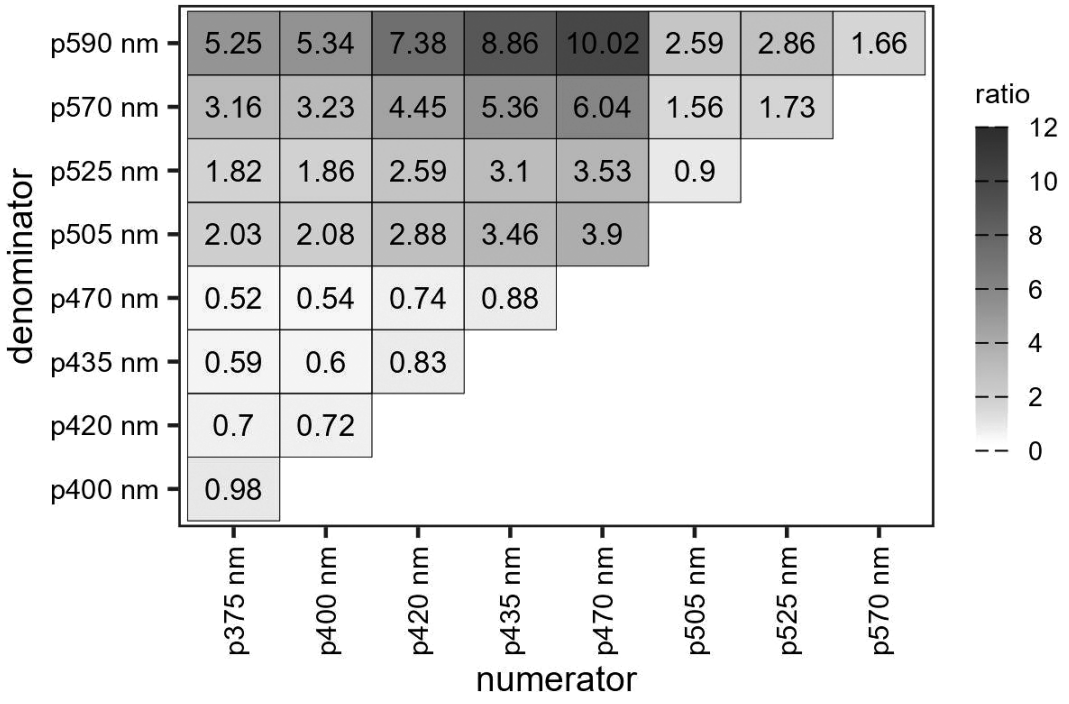

Fig. 2. Fluorescence ratio of *Karenia* bloom water
Karenia bloom water was collected on 2 November 2021 from the Katsurakoi fishing port. In total, 36 fluorescence value ratios were obtained using the Multi-Exciter.

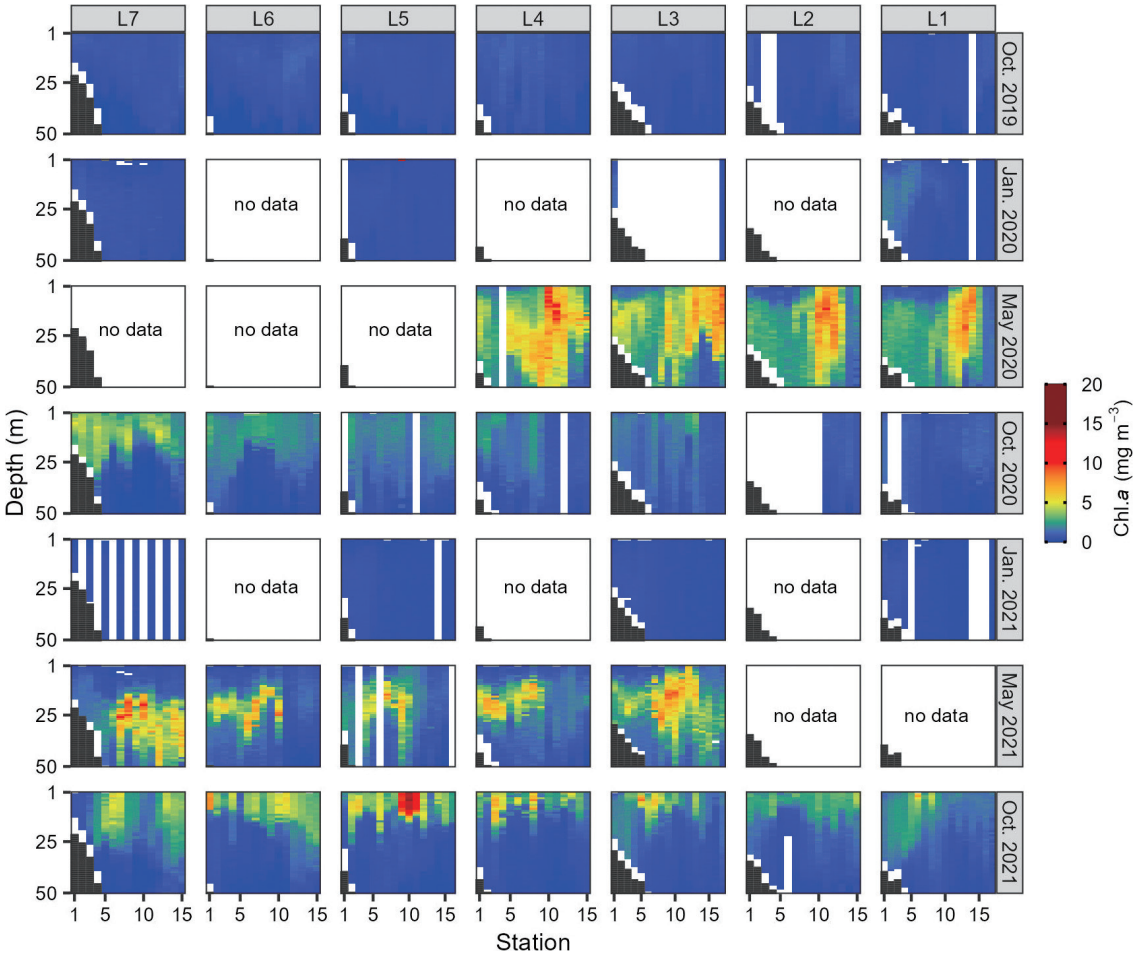

Fig. 3. Vertical distribution of Chl. *a*

The concentration of Chl. *a* was estimated from the value excited at 435 nm of the multi-wavelength excitation fluorometer. The station numbers are shown at the bottom of the figure. The dark gray color indicates the seafloor.

2. Phytoplankton community structure

The ratio of the phytoplankton group in the L3-line showed clear seasonal variation (Fig. 4). Diatoms in winter (January) and spring (May) were dominant at stations where Chl. *a* concentrations were high. However, the ratio of phytoplankton groups was different each year in autumn (October). The proportions of other phytoplankton, cyanophytes, and diatoms were approximately 40%, 30%, and 20%, respectively, in 2019. The proportions of dinoflagellates and cryptophytes were approximately 5%. Diatoms were dominant at many stations in 2020, contributing to 50% of the Chl. *a* concentrations. The ratios of the other four groups were the lowest over the three years. In 2021, the proportion of diatoms was less than 20%, and that of other phytoplankton increased to approximately 50%. The dinoflagellates and cryptophytes also increased in proportion, but neither exceeded 10%.

3. Detection of *Karenia* blooms

The *Karenia* bloom water was dark brown, the cell density of *Karenia* spp. was 17,920 cells mL^{-1}, and no other phytoplankton was detected. The *Karenia*-specific pigment gyroxanthin-diester was detected using HPLC analysis of *Karenia* bloom water (Fig. 5). In addition, diatom-containing pigments (Chl. c_2, fucoxanthin, diadinoxanthin) and 19'-butanoyloxyfucoxanthin, which are found in Haptophyceae (Prymnesiophyceae) and Chrysophyceae (Jeffrey & Vesk 1997), were also detected. Peridinin, a marker pigment of the Dinophyceae, was not detected.

From October 2019 to May 2021, *Karenia* spp. were scarce and their concentration was low (< 1,000 cells L^{-1}) during observation. A high density (> 10,000 cells L^{-1}) of *Karenia* spp. was observed in the L-lines in October 2021 (Fig. 6, Kuroda et al. 2021), when a red tide occurred in this region (Iwataki et al. 2022).

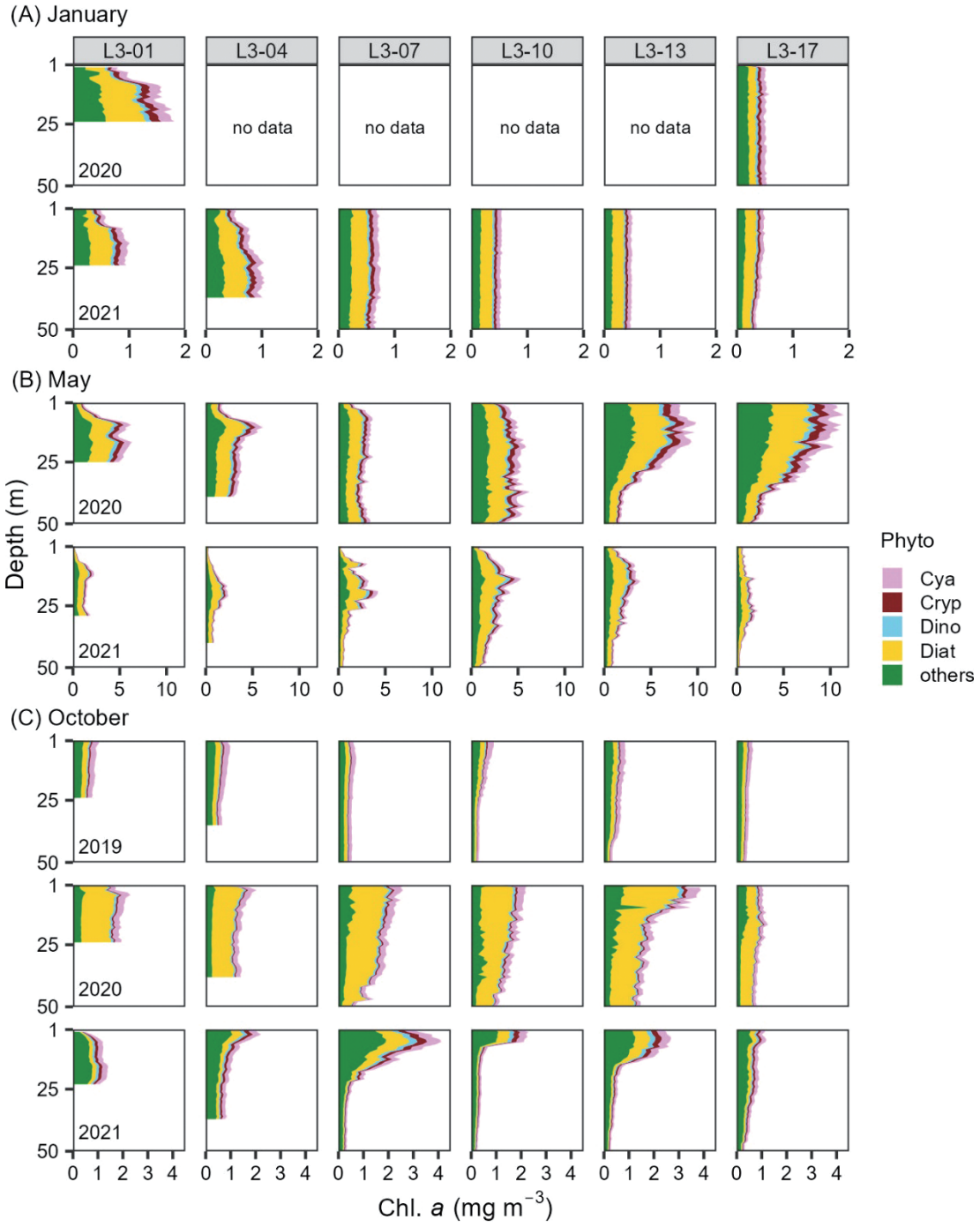

Fig. 4. Phytoplankton composition at L3-line

The concentration of Chl. *a* in the L3-line was estimated as detailed in Figure 2. The colored area shows the composition of the Phytoplankton group (Cya: cyanobacteria, Cryp: cryptophytes, Dino: dinoflagellates, Diat: diatoms, others: other phytoplankton).

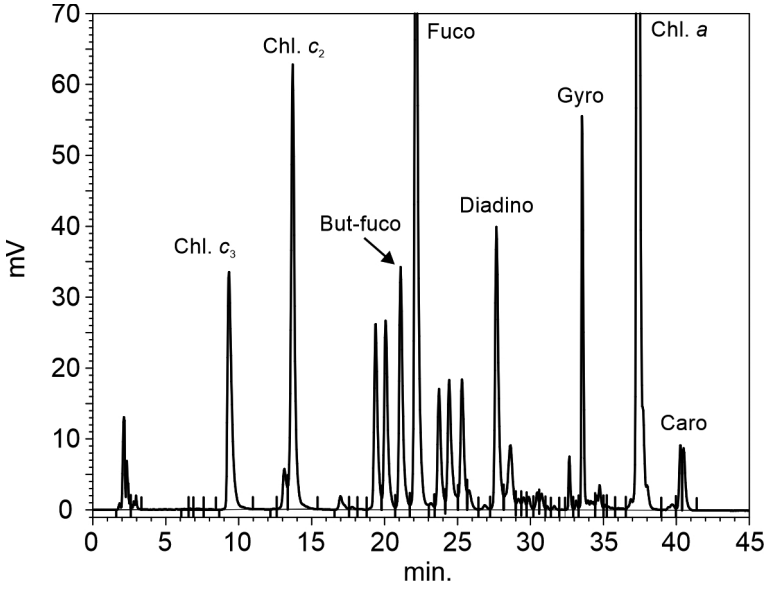

Fig. 5. HPLC chromatogram of *Karenia* bloom water
Karenia bloom water was collected on 2 November 2021 from the Katsurakoi fishing port. Pigments detected in *Karenia* bloom water are Chlorophyll c_3 (Chl. c_3), Chlorophyll c_2 (Chl. c_2), 19'-Butanoyloxyfucoxanthin (But-fuco), fucoxanthin (Fuco), diadinoxanthin (Diadino), gyroxanthin-diester (Gyro), Chlorophyll *a* (Chl. *a*), and Carotene (Caro).

A high *Karenia* index (> 2.28) was observed in all lines during the *Karenia* outbreak period (October 2021) (Fig. 7). The sea bottom depth was 50 m-200 m at stations showing a high *Karenia* index, and a high *Karenia* index was observed at depths of 1 m-20 m. The *Karenia* index from October 2019 to May 2020 and January 2021 was < 2.5. However, a high *Karenia* index was observed offshore at the L7-line at a depth of 10 m-50 m in October 2020 and May 2021.

Figure 8 shows the fluorescence ratios at 5 and 25 m for L7-15 in January, May, and October 2021. In January, when the *Karenia* index was low, the ratio of fluorescence values given by 435:590 nm was the highest at approximately 4.5. In May, the highest values at both 5 and 25 m (5.78 and 10.61, respectively) were found at the ratio of fluorescence values given by 470:590 nm. The ratio of fluorescence values given by 470:570 nm was also high (5.98) at 25 m in May, with a *Karenia* index > 2.28. The ratio of fluorescence values at 470:590 nm was highest at both depths (9.9 at 5 m and 9.06 at 25 m) in October. The ratio of fluorescence values at 470:570 nm was also high at both depths (5.84 at 5 m and 5.14 at 25 m).

Discussion

We used MEX to determine the horizontal and vertical distributions of phytoplankton composition at high resolution. In January, the phytoplankton distribution was vertically uniform due to the vertical mixing that occurs during winter (Fig. 4A). Chl. *a* concentrations were high in May, and diatoms were dominant (Fig. 4B), suggesting that a spring bloom had occurred. This was consistent with previous reports that spring blooms are caused by diatoms (Shinada et al. 2001, Hattori-Saito et al. 2010). High Chl. *a* concentrations were observed off the coast and were distributed up to 35 m from the surface layer, indicating that the blooms were not limited to the surface layer. This result indicated that MEX can be applied to conveniently investigate the vertical profile of phytoplankton community structure when diatoms are dominant, as reported by Kodama et al. (2022). Chl. *a* concentration and phytoplankton composition differed between October 2019 and 2020. Greater fluctuations were observed in October than in the other months. These fluctuations may be attributed to the influence of various water masses, such as the modified Soya Warm Current water and Oyashio water (Kusaka et al. 2013).

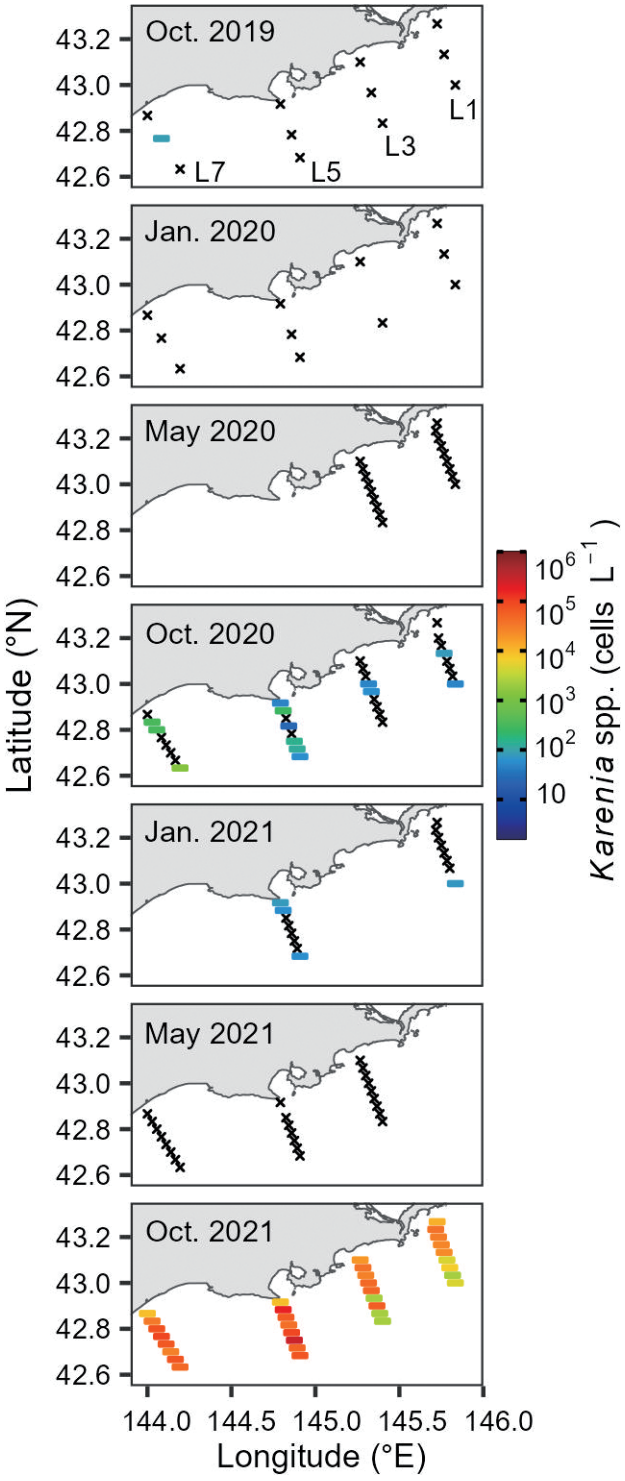

Fig. 6. Abundance of *Karenia* spp.
The cell density of *Karenia* spp. was counted under a microscope. Water samples were collected at 10 m depth except in L1-05 in January 2021, where it was collected at 0 m. The stations where no *Karenia* spp. were found are shown as cross mark.

In October 2021, Chl. *a* concentration was as high as that in May, and it was distributed in the surface layer from depths of 0 to 20 m (Fig. 3). The major phytoplankton composition detected using MEX in October 2021 comprised other phytoplankton (Fig. 4C), but high Chl. *a* concentrations were ascribed to the *Karenia* outbreak (Iwataki et al. 2022, Kuroda et al. 2021, Taniuchi et al. 2023). This is because *K. selliformis* contains almost no peridinin, an indicator pigment for dinoflagellates, but contains gyroxanthin-diester, fucoxanthin, and diadinoxanthin, which are found in diatoms (Mardones et al. 2020). Therefore, from the perspective of pigment analysis, *Karenia* spp. were not grouped as dinoflagellates using MEX, but were classified as other phytoplankton.

We could not precisely detect the *Karenia* (dinoflagellate) bloom during the *Karenia* outbreak (October 2021) using the standard MEX method. Yentsch & Yentsch (1979) suggested that the fluorescence ratio is useful for analyzing phytoplankton composition, and Proctor & Roesler (2010) conducted subsequent experiments. In this study, 36 combinations of *Karenia* bloom fluorescence ratios were obtained from *Karenia* bloom water and were used as reference data to detect *Karenia* blooms in the field. The fluorescence ratio of *Karenia* bloom water was high at fluorescence values given by 470:590 nm and 470:570 nm (Fig. 2). This is because *Karenia* spp. lack pigments that excite at 570 and 590 nm, and contain pigments that are excited at 435 nm and 470 nm. In the present study, a high *Karenia* index (> 2.28) was observed in all observation lines in October 2021 (Fig. 7). This strongly suggested that similar fluorescence properties of *Karenia* bloom waters in Katsurakoi were observed in all observation lines in October 2021.

A high *Karenia* index was also detected at a depth of 9 m at station L7-14 in October 2020 (Fig. 7). The cell density of the *Karenia* spp. at this station was unknown, as no water was collected for microscopic observation; however, low-density *Karenia* spp. cells were detected using microscopic observation in L7-15 at the next station of L7-14 (Fig. 6). It is possible in this instance that the *Karenia* index provided a reliable indication.

A high *Karenia* index was observed in the offshore region of the L7-line at a depth of 20 m-50 m below the euphotic layer in May 2021 (Fig. 7). The fluorescence ratio of fluorescence values given by 470:590 nm and 590:470 nm at 25 m was high in May 2021 (Fig. 8D), as was that of October 2021 (Fig. 8F) and the reference data of the *Karenia* bloom water (Fig. 2). We cannot reject the possibility that *Karenia* spp. were present in this layer in May 2021; however, we cannot ignore the possibility of misidentification. The cell density of *Karenia* spp. at 10

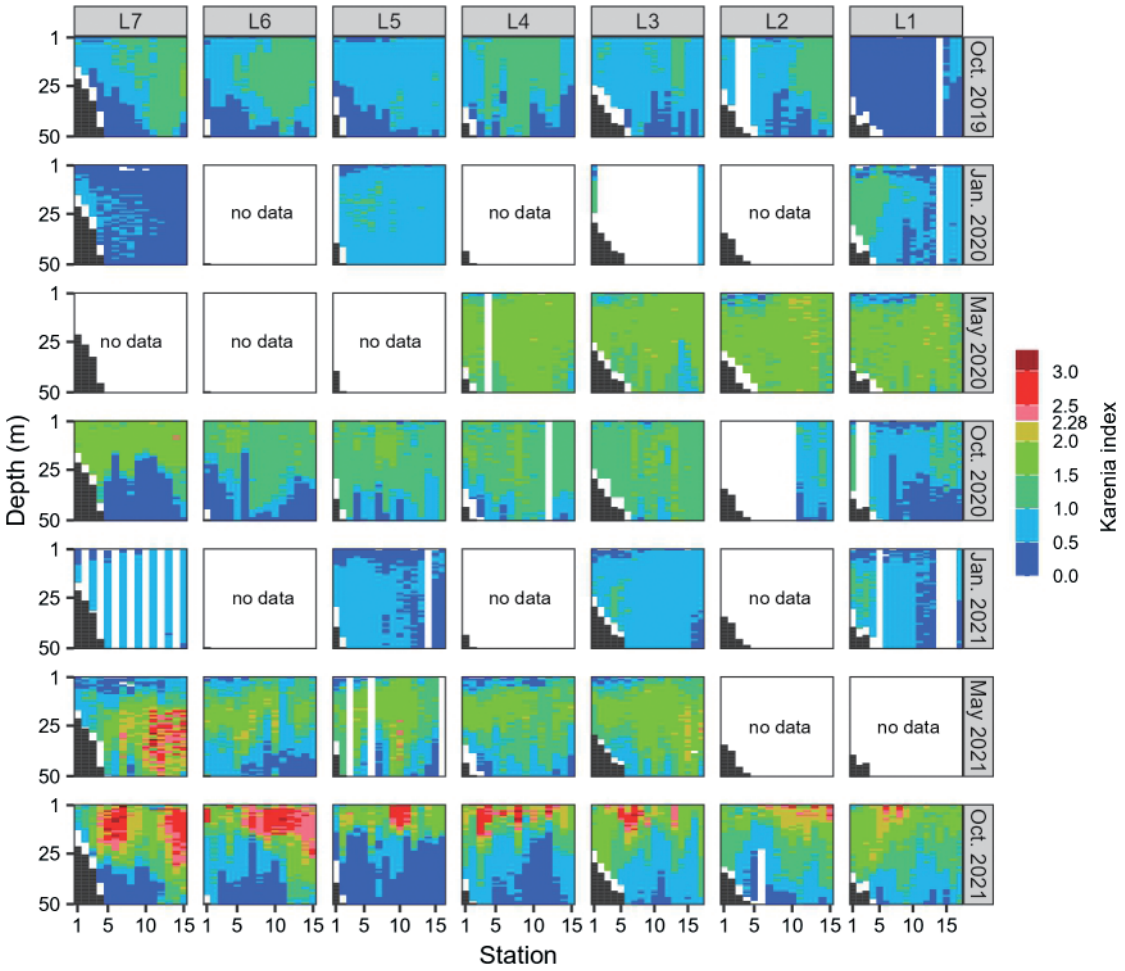

Fig. 7. Vertical distribution of *Karenia* index
The *Karenia* index was estimated from the similarity of the fluorescence properties when *Karenia* bloom water was compared with the observation results. The number of lines is shown at the top of the figure. The station numbers are shown at the bottom of the figure. The dark gray color indicates the seafloor.

m counted under the microscope was below the detection limit (Fig. 6). Additionally, the major phytoplankton composition detected using MEX showed that the proportion of diatoms in May 2021 was high at 50%, whereas that of other phytoplankton (*Karenia* spp. were classified in this group in October 2021) was not as high as that during the red tide in October 2021 (Fig. 4). The distribution of the *Karenia* index is inconsistent with the previously reported vertical migration of *Karenia* spp. Koizumi et al. (1996) showed that *K. mikimotoi* was distributed in the surface layer in the morning. Our observations at the L7-line in May 2021 began at sunrise. However, the *Karenia* index at the surface layer was lower than that at 20 m-50 m. Thus, when high *Karenia* indices are detected, they need to be scrutinized regarding microscopic observations and environmental conditions.

The cell densities of *Karenia* spp. in October 2021 were high in all stations of the L5-line where microscopic observations were made (Fig. 5). However, the *Karenia* indices of L5-05, L5-07, L5-13, and L5-15 were < 2.28 (Fig. 6), indicating that the bloom of *Karenia* spp. may have been underestimated. Therefore, it must be used in conjunction with regular microscopic observations for accurate monitoring.

Although the *Karenia* bloom could be misidentified using MEX, stations with a high *Karenia* index were present on the continental shelf, which is consistent with a previous report (Kuroda et al. 2021). Moreover, a high *Karenia* index was observed at depths of 1 m-20 m. The depth of the euphotic layer in October was 17.6 ± 10.4 m; thus, the *Karenia* spp. blooms were widespread in the euphotic layer. This was consistent with previous reports

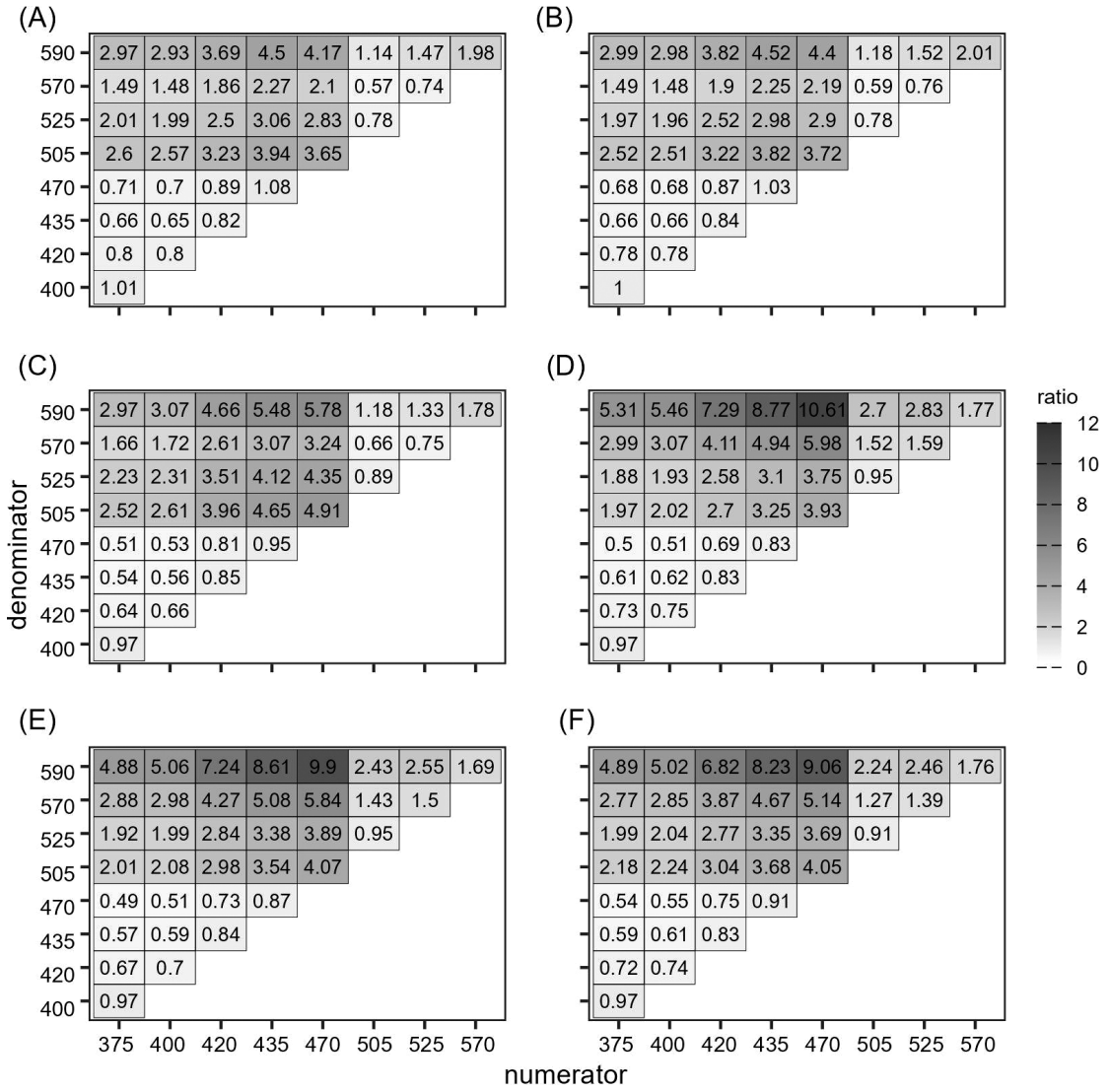

Fig. 8. Fluorescence ratio at 5 and 25 m of L7-15 in 2021

In total, 36 fluorescence value ratios were obtained using Multi-Exciter at 5 m (A, C, E) and 25 m (B, D, F), in January (A, B), May (C, D), and October (E, F) in 2021.

that *K. mikimotoi* is distributed in the euphotic layer during the day (Honjo et al. 1990, Yamaguchi 1994, Koizumi et al. 1996, Miyamura 2016). Furthermore, as *Karenia* migrate vertically (Gillibrand et al. 2016), we assumed that they were distributed more deeply at night. *Karenia* outbreaks have also affected benthic organisms, resulting in a decrease in sea urchins living on the seabed in coastal areas (Johnstone et al. 2024) and shellfish living in the intertidal zone (Yao & Noda 2023) and the death of whelks (Misaka & Ando 2021). Our results indicated that the impact of *Karenia* during the outbreaks reached a depth of 20 m. Thus, it is possible that the *Karenia* outbreaks affected benthic organisms in both the tidal and neritic zones (sea bottom < 20 m). The neritic zone is not as wide off the coast of eastern Hokkaido but spreads several kilometers from the coastline; thus, the impact of *Karenia* outbreaks on benthic ecosystems may be larger than observed onshore.

In conclusion, in this study, we examined the phytoplankton community structure in southeastern Hokkaido from 2019 to 2021. Although some misidentification issues occurred regarding taxa owing to pigment characteristics, we understood the general community structure, and our method was more useful for capturing subsurface Chl. *a* maximum and minute changes than having to sample water from each layer. We also attempted to detect the fluorescence properties of *Karenia* blooms using MEX. The advantage of this

method is that *Karenia* spp. can be detected in parallel with phytoplankton community monitoring without any new settings in MEX. This method is expected to aid in the prescreening of *Karenia* blooms; however, the species responsible for the bloom must be observed microscopically when the *Karenia* index > 2.0. The number of reference samples must be increased, and a combination of the *Karenia* index and other pertinent factors, such as phytoplankton composition, must be considered to improve detection using MEX, as described by Kodama et al. (2022).

Acknowledgements

We thank the crew of R/Vs *Hokko-maru* and *Wakataka-maru* for monitoring the L-lines. We are also grateful to Hiromi Kasai, Hiroshi Kuroda, Takuya Nakanowatari, and Takuya Ohnishi for supporting the MEX observations, and Mitsunori Iwataki and Kazuya Takahashi for their aid in the HPLC analysis; and Natsuki Hasegawa for sampling *Karenia* bloom water. This study was partially supported by the Fisheries Resources Institute of the Japan Fisheries Research and Education Agency.

References

Alexanin, A. et al. (2023) Methodology and results of satellite monitoring of *Karenia* microalgae blooms, that caused the ecological disaster off Kamchatka Peninsula. *Remote Sens.*, **15**, 1197.

Bjørnsen, P. K. & Nielsen, T. G. (1991) Decimeter scale heterogeneity in the plankton during a pycnocline bloom of *Gyrodinium aureolum*. *Mar. Ecol. Prog. Ser.*, **73**, 263-267.

Dodson, A. N. & Thomas, W. H. (1964) Concentrating plankton in a gentle fashion. *Limnol. Oceanogr.*, **9**, 455-456.

GEOHAB (2010) Global ecology and oceanography of harmful algal blooms, harmful algal blooms in Asia. *In* Furuya, K. et al. (eds), Harmful algal blooms in Asia: a regional comparative programme, IOC and SCOR, Paris and Newark, Delaware, p. 68.

Gillibrand, P. A. et al. (2016) Individual-based modelling of the development and transport of a *Karenia mikimotoi* bloom on the North-west European continental shelf. *Harmful Algae*, **53**, 118-134.

Hasegawa, N. et al. (2022) Repeated reaching of the harmful algal bloom of *Karenia* spp. around the Pacific shoreline of Kushiro, eastern Hokkaido, Japan, during autumn 2021. *Fish. Sci.*, **88**, 787-803.

Hattori-Saito, A. et al. (2010) Iron deficiency in micro-sized diatoms in the Oyashio region of the Western subarctic Pacific during spring. *J. Oceanogr.*, **66**, 105-115.

Honjo, T. et al. (1990) Annual cycle of motile cells of *Gymnodinium nagasakiense* and ecological features during the period of red tide development. *In* Granéli, E. et al. (eds), Toxic marine phytoplankton, Elsevier, New York, pp. 165-170.

Iwataki, M. et al. (2022) Morphological variation and phylogeny of *Karenia selliformis* (Gymnodiniales, Dinophyceae) in an intensive cold-water algal bloom in eastern Hokkaido, Japan. *Harmful Algae*, **114**, 102204.

Jeffrey, S. W. & Vesk, M. (1997) Introduction to marine phytoplankton and their pigment signatures. *In* Jeffrey, S. W. et al. (eds), Phytoplankton pigments in oceanography, UNESCO, Paris, pp. 261-264.

Johnstone, J. et al. (2024) The effect of a harmful algal bloom (*Karenia selliformis*) on the benthic invertebrate community and the sea otter (*Enhydra lutris*) diet in eastern Hokkaido. *PLOS One*, 2024.04.23.590716, **19**, e0303126.

Kakumu, A. et al. (2018) First detection of the noxious red tide dinoflagellate *Karenia mikimotoi* and bloom dynamics in 2015 and 2016 in Hakodate Bay, Hokkaido, northern Japan. *Nihon Purankuton Gakkai Ho* (*Bull. Plankton Soc. Jpn.*), **65**, 1-11 [In Japanese with English abstract].

Kodama, T. et al. (2022) Empirical estimation of marine phytoplankton assemblages in coastal and offshore areas using an in situ multi-wavelength excitation fluorometer. *PLOS One*, **17**, e0257258.

Koeller, P. et al. (2009) Basin-scale coherence in phenology of shrimps and phytoplankton in the North Atlantic Ocean. *Science*, **324**, 791-793.

Koizumi, Y. et al. (1996) Diurnal vertical migration of *Gymnodinium mikimotoi* during a red tide in Hoketsu Bay, Japan. *J. Plankton Res.*, **18**, 289-294.

Kuroda, H. et al. (2021) Unprecedented outbreak of harmful algae in Pacific coastal waters off southeast Hokkaido, Japan, during late summer 2021 after record-breaking marine heatwaves. *J. Mar. Sci. Eng.*, **9**, 1335.

Kuroda, H. et al. (2022) Distribution of harmful algae (*Karenia* spp.) in October 2021 off southeast Hokkaido, Japan. *Front. Mar. Sci.*, **9**, 841364.

Kusaka, A. et al. (2013) Monthly variations of hydrographic structures and water mass distribution off the Doto area, Japan. *J. Oceanogr.*, **69**, 295-312.

Mardones, J. I. et al. (2020) Unraveling the *Karenia selliformis* complex with the description of a non-gymnodimine producing Patagonian phylotype. *Harmful Algae*, **98**, 101892.

Millie, D. F. et al. (1997) Detection of harmful algal blooms using photopigments and absorption signatures: A case study of the Florida red tide dinoflagellate, *Gymnodinium breve*. *Limnol. Oceanogr.*, **42**, 1240-1251.

Misaka, T. & Ando, Y. (2021) Hokkaido taiheiyo engan de hassei shita daikibo yuugai akashiwo ni tsuite (Huge red tide occurred in Pacific coast of Hokkaido). *Shikenkenkyu Ha Ima*, 943, Fisheries Research Dept., Hokkaido Research Organ [In Japanese].

Miyamura, K. (2016) Population dynamics, prediction and countermeasures of *Karenia mikimotoi* red tides. *In* Imai, I. et al. (eds), Advances in harmful algal bloom research, Kouseisha Kouseikaku, Tokyo, Japan, pp. 191-200 [In Japanese].

Miyazono, A. & Kuroda, H. (2024) Origin of seeds of *Karenia selliformis* red tide that occurred along the Pacific coast of Hokkaido 2021 ~ Consideration of the transportation route of the seeds from Kamchatka to eastern Hokkaido and the water temperature condition of the route ~, Hokkaido.

Hokkaido Suisan Shikenjo Kenkyu Hokoku (*Sci. Rep. Hokkaido Fish Res. Inst.*), **106**, 1-10 [In Japanese with English abstract].

Natsuike, M. et al. (2023) First occurrence and a red-tide event of harmful dinoflagellate *Karenia mikimotoi* in Funka Bay, Hokkaido. *Hokkaido Suisan Shikenjo Kenkyu Hokoku* (*Sci. Rep. Hokkaido Fish Res. Inst.*), **104**, 21-31 [In Japanese with English abstract].

Orlova, T. Y. et al. (2022) A massive bloom of *Karenia* species (Dinophyceae) off the Kamchatka coast, Russia, in the fall of 2020. *Harmful Algae*, **120**, 102337.

Örnólfsdóttir, E. B. et al. (2003) Quantification of the relative abundance of the toxic dinoflagellate, *Karenia brevis* (Dinophyta), using unique photopigments. *J. Phycol*., **39**, 449-457.

Platt, T. et al. (2003) Spring algal bloom and larval fish survival. *Nature*, **423**, 398-399.

Proctor, C. W. & Roesler, C. S. (2010) New insights on obtaining phytoplankton concentration and composition from in situ multispectral Chlorophyll fluorescence. *Limnol. Oceanogr.*, **8**, 695-708.

Sakamoto, S. et al. (2021) Harmful algal blooms and associated fisheries damage in East Asia: Current status and trends in China, Japan, Korea and Russia. *Harmful Algae*, **102**, 101787.

Shikata, T. et al. (2017) Relationships between light environment and subsurface accumulation during the daytime in the red-tide dinoflagellate *Karenia mikimotoi*. *Mar. Biol*., **164**, 18.

Shimada, H. et al. (2016) First record of red tide due to the harmful dinoflagellate *Karenia mikimotoi* in Hakodate Bay, southern Hokkaido, in autumn 2015. *Nippon Suisan Gakkaishi* (*J. Jpn. Soc. Fish. Sci*.), **82**, 934-938 [In Japanese with English abstract].

Shinada, A. et al. (2001) Seasonal dynamics of planktonic food chain in the Oyashio region, western subarctic Pacific. *J. Plankton Res.*, **23**, 1237-1248.

Sildever, S. et al. (2019) Toxic HAB species from the Sea of Okhotsk detected by a metagenetic approach, seasonality and environmental drivers. *Harmful Algae*, **87**, 101631.

Taniuchi, Y. et al. (2023) Drastic changes in a lower-trophic-level ecosystem attributed to unprecedented harmful algal outbreaks in 2021 on the Pacific shelf off southeast Hokkaido, Japan. *Cont. Shelf Res.*, **267**, 105114.

Yamaguchi, A. et al. (2022) Horizontal distribution of harmful red-tide *Karenia selliformis* and phytoplankton community along the Pacific coast of Hokkaido in autumn 2021. *Suisan kaiyo kenkyu* (*Bull. Jpn. Soc. Fish. Oceanogr.*), **86**, 41-49 [In Japanese with English abstract].

Yamaguchi, M. (1994) Physiological ecology of the red tide flagellate *Gymnodinium nagasakiense* (Dinophyceae): mechanism of the red tide occurrence and its prediction. *Nanseikaiku suisankenkyujo kenkyuhoukoku* (*Bull. Nansei Natl. Fish. Res. Inst.*), **27**, 251-394 [In Japanese with English abstract].

Yao, Y. & Noda, T. (2023) Immediate impact of the 2021 harmful algal bloom in southeast Hokkaido on the rocky intertidal community and its spatial variation. *bioRxiv*, 2023.12.01.569513.

Yentsch, C. S. & Yentsch, C. M. (1979) Fluorescence spectral signatures: the characterization of phytoplankton populations by the use of excitation and emission spectra. *J. Mar. Res*., **37**, 471-483.

Yoshida, M. et al. (2021) A new fluorometer to detect harmful algal bloom species and its application as a long–term HABs monitoring tool. *J. Fac. Agric. Kyushu Univ.*, **66**, 37-43.

Yoshida, M. et al. (2011) In situ multi-excitation chlorophyll fluorometer for phytoplankton measurements: technologies and applications beyond conventional fluorometers. OCEANS'11 MTS/IEEE KONA, Waikoloa, pp. 1-4.

Zapata, M. et al. (2000) Separation of chlorophylls and carotenoids from marine phytoplankton: a new HPLC method using a reversed phase C_8 column and pyridine-containing mobile phases. *Mar. Ecol. Prog. Ser.*, **219**, 85-98.